Supplementary Tables

Supplementary Table 1. Small molecule screening data

Category	Parameter	Description
Assay	Type of assay	Competition with FP-TMR binding
	Target	Multiple active hydrolases in live *S. aureus*
	Primary measurement	Fluorescence scan after SDS-PAGE analysis of probe-labeled lysate
	Key reagents	FP-TMR
	Assay protocol	*S. aureus* ATCC3556 was plated out on TSAMg and grown for 48-72 hours. Cells were scraped off plates and resuspended in TSB at OD_{600} of 60-100. 0.5 μL of each of 7 compounds of serine-reactive compound library (1 mM in DMSO) were pooled in a microtube and 46 μL of the bacterial suspension were added. Samples were incubated at 37 °C, 300 rpm for 60 min and 1 μL of FP-TMR (50 μM stock in DMSO) was added. After 30 min incubation at 37 °C, samples were centrifuged and the supernatant discarded. Bacterial pellets were resuspended in 400 μL ice-cold PBS/0.1% SDS, lysed by bead-beating and analyzed by SDS-PAGE.
	Additional comments	-
Library	Library size	~500
	Library composition	Small molecules with serine-reactive electrophiles
	Source	Bogyo Lab, Stanford University
	Additional comments	-
Screen	Format	12 microtubes per 96 well plate, multiplexed
	Concentration(s) tested	10 μM
	Plate controls	DMSO, Non-fluorescent probe analog FP-biotin
	Reagent/ compound dispensing system	Manual
	Detection instrument and software	Typhoon 9410 variable mode imager (TAMRA channel, λ_{ex} = 380, 580 BP filter) with Typhoon Scanner Control v 5.0 software
	Assay validation/QC	-
	Correction factors	-
	Normalization	-
	Additional comments	Individual compounds of active pools were rescreened. Compounds showing >50% competition with FP-TMR of at least one band were tested in dose-response (100 μM – 160 nM)
Post-HTS analysis	Hit criteria	>90% inhibition of one hydrolase with no detectable activity against secondary targets at any concentration in the dose-response curve
	Hit rate	1.8%
	Additional assay(s)	-
	Confirmation of hit purity and structure	LC-MS
	Additional comments	-

Supplementary Table 2. List of serine hydrolases identified by LC/LC-MS/MS analysis

Gene	Previous annotation	Mw (DA), full length	strain NCTC8325 gene locus tag	strain Newman locus tag	strain USA300 locus tag
gehA[27]	*S. aureus* lipase 1 (SAL1)	76675	SAOUHSC_03006	NWMN_2569	SAUSA300_2603
gehB[27]	*S. aureus* lipase 2 (SAL2)	76388	SAOUHSC_00300	NWMN_0262	SAUSA300_0320
fphA	Para-nitrobenzyl esterase	51969	SAOUHSC_02751	NWMN_2350	SAUSA300_2396
fphB	Acetyl esterase/lipase	36848	SAOUHSC_02844	NWMN_2434	SAUSA300_2473
fphC	Alpha/beta hydrolase	35256	SAOUHSC_01279	NWMN_1210	SAUSA300_1194
fphD	Alpha/beta hydrolase	33186	SAOUHSC_02448	NWMN_2092	SAUSA300_2148
fphE	Hydrolase family protein; H30[6]	31006	SAOUHSC_02900	NWMN_2480	SAUSA300_2518
fphF	Putative tributyrin esterase	29096	SAOUHSC_02962	NWMN_2528	SAUSA300_2564
fphG	Alpha/beta hydrolase	28362	SAOUHSC_01912	NWMN_1683	SAUSA300_1733
fphH	Carboxylesterase; E28[6]	28094	SAOUHSC_00802	NWMN_0784	SAUSA300_0763
fphI	Carboxylesterase	27443	SAOUHSC_00417	NWMN_0422	SAUSA300_0430
fphJ	Phospholipase/carboxylesterase family protein	21783	SAOUHSC_02824	NWMN_2416	SAUSA300_2457

Supplementary Table 3. Bioinformatic analyses of FphB protein sequence

Tool	Result
SignalP	No signal peptide
Secretome P2.0	Not secreted
psortb v 3.0	Localization scores: Cytoplasmic 7.50; Cytoplasmic membrane 1.15 Extracellular 0.73 Cell wall 0.62
Phobius	N-terminus cleaved after amino acid 18
Signal3L-2.0	Cleave site after amino acid 18 (Score=1). Input sequence does not include a signal peptide, but may include a N-terminal transmembrance helix (TMH).
MemBrain	N-terminal signal peptide: not detected; Predicted Transmembrane Helix (TMH): #1 TMH: 7-18 (possible half-TMH)
TmPred	STRONGLY preferred model: N-terminus inside, 1 strong transmembrane helices from amino acid 5 - 20, total score : 1004

Supplementary Table 4. Bacterial strains used in this study

Strain	Description	Reference/Source
S. aureus ATCC3556	Restriction-deficient mutant derived from strain NCTC 8325, MSSA, biofilm-forming	[52,53]
S. aureus strain Newman	Wild-type clinical osteomyelitis isolate	[54]
S. aureus strain Newman-pCM29	WT Newman strain with GFP plasmid pCM29; Cm^R	Plasmid in [51].This work.
NWMN_SAL1::$\phi N\sum$ (NWMN_2569::$\phi N\sum$)	Transposon insertion mutant in NWMN_2569 (SAL1); Ery^R, $Linc^R$	This work
NWMN_SAL2:: $\phi N\sum$ (NWMN_0262:: $\phi N\sum$)	Transposon insertion mutant in NWMN_0262 (*lip2*, SAL2)); homolog to SAUSA300_0320, SAOUHSC00300 Ery^R, $Linc^R$	This work
NWMN_*fph*A:: $\phi N\sum$ (NWMN_2350::$\phi N\sum$)	Transposon insertion mutant in NWMN_2350 (*fph*A/*pnb*A); homolog to SAUSA300_2396, SAOUHSC_02751; Ery^R, $Linc^R$	This work
NWMN_*fphB*::$\phi N\sum$ (NWMN_2434::$\phi N\sum$)	Transposon insertion mutant in NWMN_2434 (*fphB*); homolog to SAOUHSC_02844, SAUSA300_2473 Ery^R, $Linc^R$	This work
NWMN_*fph*C::$\phi N\sum$ (NWMN_1210::$\phi N\sum$)	Transposon insertion mutant in NWMN_1210 (*fph*C); homolog to SAUSA300_1194, SAOUHSC_01279 Ery^R, $Linc^R$	This work
NWMN_*fph*D::$\phi N\sum$ (NWMN_2092::$\phi N\sum$)	Transposon insertion mutant in NWMN_2092 (*fph*D); homolog to SAUSA300_2148, SOUHSC_02448 Ery^R, $Linc^R$	This work
NWMN_*fph*E::$\phi N\sum$ (WMN_2480::$\phi N\sum$)	Transposon insertion mutant in NWMN_2480 (*fph*E); homolog to SAUSA300_2518, SAOUHSC_02900 Ery^R, $Linc^R$	This work
NWMN_*fph*F::$\phi N\sum$ (NWMN_2528::$\phi N\sum$)	Transposon insertion mutant in NWMN_2528 (*fph*F/*est*A); homolog to SAUSA300_2564, SAOUHSC_02962; Ery^R, $Linc^R$	This work
NWMN_*fph*G::$\phi N\sum$ (NWMN_1683::$\phi N\sum$)	Transposon insertion mutant in NWMN_1683 (*fph*G); homolog to SAUSA300_1733, SOUHSC_01912 Ery^R, $Linc^R$	This work
NWMN_*fph*H::$\phi N\sum$ (NWMN_0784::$\phi N\sum$)	Transposon insertion mutant in NWMN_0784 (*fph*H); homolog to SAUSA300_0763, SAOUHSC_00802 Ery^R, $Linc^R$	This work
NWMN_0169::$\phi N\sum$	Transposon insertion mutant in NWMN_0169; homolog to SAUSA300_0227 Ery^R, $Linc^R$	This work
NWMN_2379::$\phi N\sum$	Transposon insertion mutant in NWMN_2379; homolog to SAUSA300_2424 and SOUHSC02783 Ery^R, $Linc^R$	This work

USA300 LAC	Wild-type USA300 Los Angeles County (LAC) clone; multilocus sequence type 8, SCCmec type IV cured of antibiotic resistance plasmid	[55]
SAUSA300_0227*::* $\phi N\sum$	Transposon insertion mutant in SAUSA300_0227; Ery^R, $Linc^R$	Nebraska Transposon Mutant Library
SAUSA300_0320*::*$\phi N\sum$	Transposon insertion mutant in SAUSA300_0320; Ery^R, $Linc^R$	Nebraska Transposon Mutant Library
SAUSA300_0763*::*$\phi N\sum$	Transposon insertion mutant in SAUSA300_0763; Ery^R, $Linc^R$	Nebraska Transposon Mutant Library
SAUSA300_1194*::*$\phi N\sum$	Transposon insertion mutant in SAUSA300_1194; Ery^R, $Linc^R$	Nebraska Transposon Mutant Library
SAUSA300_1733*::*$\phi N\sum$	Transposon insertion mutant in SAUSA300_1733; Ery^R, $Linc^R$	Nebraska Transposon Mutant Library
SAUSA300_2148*::*$\phi N\sum$	Transposon insertion mutant in SAUSA300_2148; Ery^R, $Linc^R$	Nebraska Transposon Mutant Library
SAUSA300_2396*::*$\phi N\sum$	Transposon insertion mutant in SAUSA300_2396; Ery^R, $Linc^R$	Nebraska Transposon Mutant Library
SAUSA300_2424*::*$\phi N\sum$	Transposon insertion mutant in SAUSA300_2424; Ery^R, $Linc^R$	Nebraska Transposon Mutant Library
SAUSA300_2473*::*$\phi N\sum$	Transposon insertion mutant in SAUSA300_2473; Ery^R, $Linc^R$	Nebraska Transposon Mutant Library
SAUSA300_2518*::*$\phi N\sum$	Transposon insertion mutant in SAUSA300_2518; Ery^R, $Linc^R$	Nebraska Transposon Mutant Library
SAUSA300_2603*::*$\phi N\sum$	Transposon insertion mutant in SAUSA300_2473; Ery^R, $Linc^R$	Nebraska Transposon Mutant Library
S. epidermidis	Wild-type strain	From Elizabeth Joyce, UCSF
L. monocytogenes 10403S pMP4 (inlA11-1Topo)	HF HS pfu ultra and primer 1 /2 amplified inlA from DH-L-1039 (10403S GFP)	[56]
H. pylori G27MA	MDCK-adapted strain from G27 wild type (isolated from patient with peptic ulcer disese)	[57]
E. coli K12 (MG1655)	F-, λ^-, *rph-1*	Coli Genetic Stock Center at Yale University
S. typhimurium SL1344	Wild-type strain	[60]

REFERENCES

51. Pang, Y. Y. *et al.* agr-Dependent interactions of *Staphylococcus aureus* USA300 with human polymorphonuclear neutrophils. *J Innate Immun* **2**, 546-559, doi:10.1159/000319855 (2010).

52. Gross, M., Cramton, S. E., Gotz, F. & Peschel, A. Key role of teichoic acid net charge in *Staphylococcus aureus* colonization of artificial surfaces. *Infect Immun* **69**, 3423-3426, doi:10.1128/IAI.69.5.3423-3426.2001 (2001).

53. Wu, J. A., Kusuma, C., Mond, J. J. & Kokai-Kun, J. F. Lysostaphin disrupts *Staphylococcus aureus* and *Staphylococcus epidermidis* biofilms on artificial surfaces. *Antimicrob Agents Chemother* **47**, 3407-3414 (2003).

54. Duthie, E. S. & Lorenz, L. L. Staphylococcal coagulase; mode of action and antigenicity. *J Gen Microbiol* **6**, 95-107, doi:10.1099/00221287-6-1-2-95 (1952).

55. Arsic, B., Zhu, Y., Heinrichs, D. E. & McGavin, M. J. Induction of the staphylococcal proteolytic cascade by antimicrobial fatty acids in community acquired methicillin resistant *Staphylococcus aureus*. *PLoS One* **7**, e45952, doi:10.1371/journal.pone.0045952 (2012).

56. Pentecost, M., Kumaran, J., Ghosh, P. & Amieva, M. R. *Listeria monocytogenes* internalin B activates junctional endocytosis to accelerate intestinal invasion. *PLoS Pathog* **6**, e1000900, doi:10.1371/journal.ppat.1000900 (2010).

57. Amieva, M. R. *et al.* Disruption of the epithelial apical-junctional complex by *Helicobacter pylori* CagA. *Science* **300**, 1430-1434, doi:10.1126/science.1081919 (2003).

58. Sanman, L. E. *et al.* Disruption of glycolytic flux is a signal for inflammasome signaling and pyroptotic cell death. *Elife* **5**, e13663, doi:10.7554/eLife.13663 (2016).

Supplementary Table 5. Oligonucleotides used in this study

Primer pair	**Sequence (5'-3')**	**Application**
SAUSA300_0227-F and R	F: TGACAGTCATCTTAGCCTCT R: AGCGTTTACAAATAAAGCGTGT	PCR confirmation of SAUSA300_0227*::* $\phi N\sum$ and successful generation of NWMN_0169*::*$\phi N\sum$
SAUSA300_0320-F and R	F: TCAACACCACAACTAAAAGTGTT R: GCCTGTCCCTTTAGTTTTCGC	PCR confirmation of SAUSA300_0320*::* $\phi N\sum$ and successful generation of NWMN_0262*::*$\varphi N\sum$
SAUSA300_0763-F and R	F: AAGTATGCAAAGGGAGCGTT R: TCATTATGCCCCTCCTTTCT	PCR confirmation of SAUSA300_0763*::*$\varphi N\sum$ and successful generation of NWMN_0748*::*$\varphi N\sum$

SAUSA300_1194-F and R	F: TGTCCTGTTTTAAGGGCATCA R: AGCAGTTGGCCCCACAATTA	PCR confirmation of SAUSA300_1194*::φNΣ* and successful generation of NWMN_1210*::φNΣ*
SAUSA300_1733-F and R	F: ACCGATCCCTAATTCAACGCA R: ACTCGCACAACGGAGTTTCT	PCR confirmation of SAUSA300_1733*::φNΣ* and successful generation of NWMN_1683*::φNΣ*
SAUSA300_2148-F and R	F: ACGACTTAGACATTTTATGGAAACT R: TGTATTCAAAATCAACTAAAGGACA	PCR confirmation of SAUSA300_2148*::φNΣ* and successful generation of NWMN_2092*::φNΣ*
SAUSA300_2396-F and R	F: AGCTCGTCTGATTCAGTCACAA R: GCACGCCTGCTATCAAATTCA	PCR confirmation of SAUSA300_2396*::φNΣ* and successful generation of NWMN_2350*::φNΣ*
SAUSA300_2424-F and R	F: TCGAACTTGTTTCTTCAGAGT R: AAATAATTTTTCGCTTTAGTTGTAA	PCR confirmation of SAUSA300_2424*::φNΣ* and successful generation of NWMN_2379*::φNΣ*
SAUSA300_2473-F and R	F: ACTCTGATAATCACTTTAGCAAGTA R: TCAGCATGGTACAGTAGAACT	PCR confirmation of SAUSA300_2473*::φNΣ* and successful generation of NWMN_2434*::φNΣ*
SAUSA300_2518-F and R	F: TGAACTGGGTTTAACAGATGAAGA R: AAGCTTGGTCAGCCATCAAA	PCR confirmation of SAUSA300_2518*::φNΣ* and successful generation of NWMN_2480*::φNΣ*
SAUSA300_2603-F and R	F: TGACTTTCCGCCAGCTTCTT R: GGATGGTCATTATGAGTGCTTGG	PCR confirmation of SAUSA300_2564*::φNΣ* and successful generation of NWMN_2569*::φNΣ*
SAOUHSC02844_Fw_BamHI	ACGAGGATCCCGTAAAAAATGGTCTACACT	Forward primer for SAOUHSC02844 cloning with BamHI site
SAOUHSC02844_Rv_XhoI	GTTTCTCGAGTTAGTTAATAATATTTTTCACTTGG	Reverse primer for SAOUHSC02844 cloning with XhoI site

Supplementary Figures

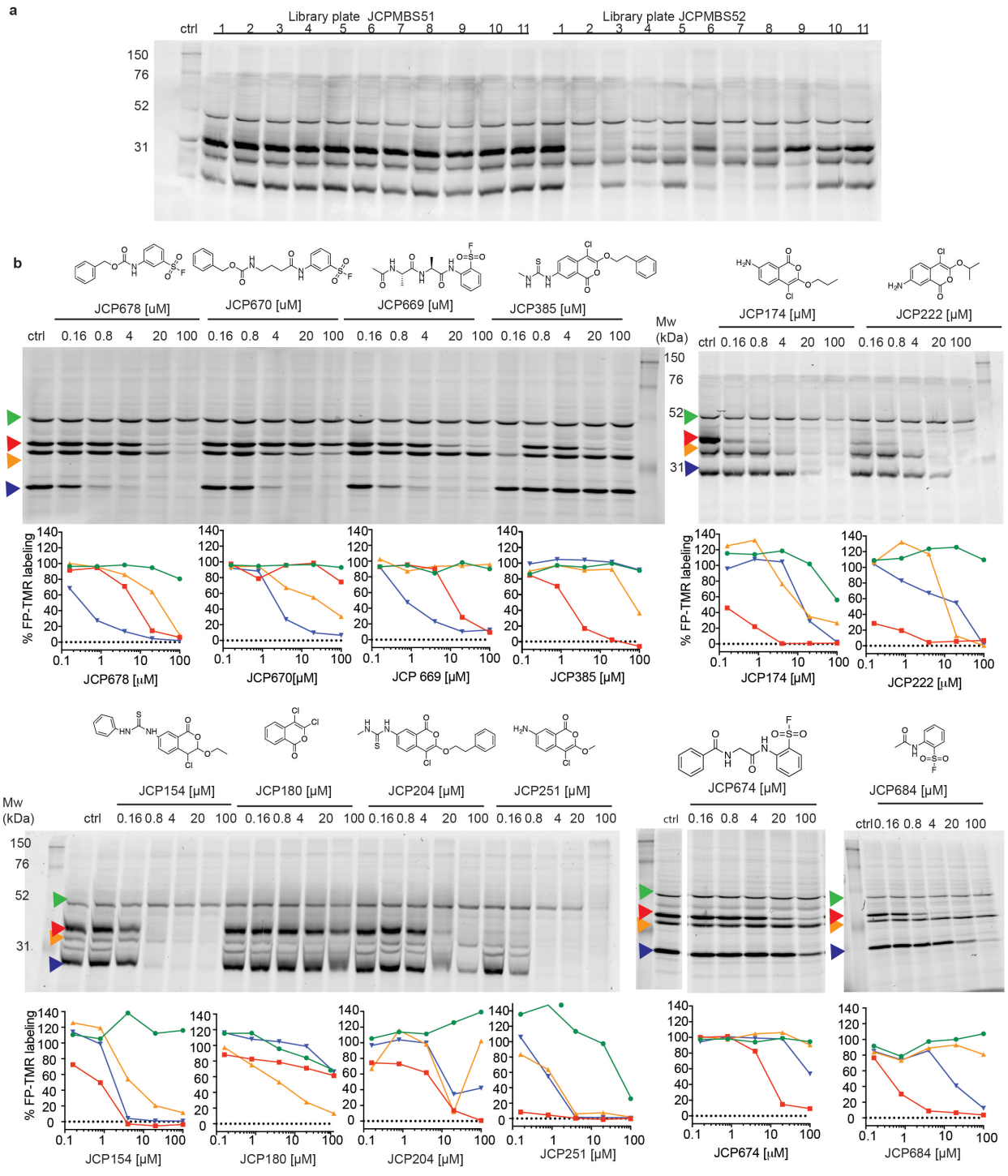

Supplementary Figure 1. Competitive activity-based protein profiling screen for inhibitors of serine hydrolases in *S. aureus*. a) SDS-PAGE gel images of samples of *S. aureus*

ATCC35556 grown on TSBMg Agar, suspended in TSB at ~OD_{600} = 50 - 100, pre-incubated with mixtures of 7 library compounds (at 10 μM each) for 60 min, and then labeled with FP-TMR (1 μM) for 30 min. Samples were lysed, separated on an SDS-gel and TMR-fluorescence imaged using a flatbed laser scanner. Exemplary data are shown from two primary screening plates. b) SDS-PAGE images of competition profiles of the indicated hit molecules after deconvolution from the pools of 7 compounds. Images show 14 individual screening hit compounds tested in dose-response for competition with FP-TMR labeling (1 μM) to evaluate potency and selectivity. Colored arrowheads indicate consistently observed serine hydrolase activities. Lower panels show quantification of FP-TMR-labeling intensities for hydrolase bands 1 (green), 2 (red: FphB), 3 (orange) and 4 (blue: FphF) in competition with the indicated compounds. Band intensities after compound pretreatment were normalized to the corresponding intensities achieved under control conditions (vehicle treatment). Band quantification was done using Image Studio Lite V 5.2.5. For JCP251 and JCP678 the experiment was performed twice with similar results, for all other compounds these dose-response curves were recorded once as part of the hit validation procedure.

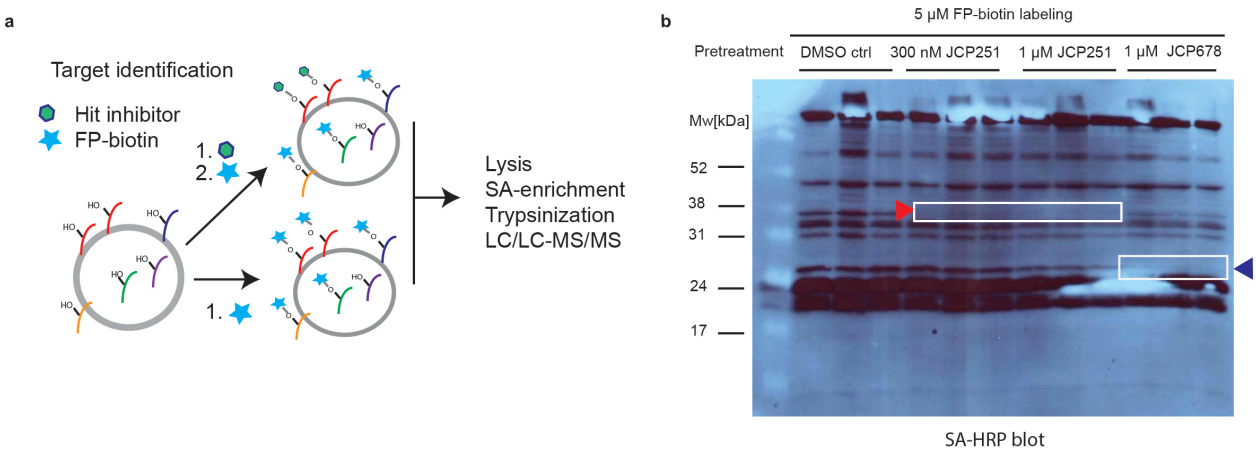

Supplementary Figure 2. Competition labeling of JCP251 and JCP678 with FP-biotin. a) Schematic representation of MS-based serine hydrolase profiling and target identification using FP-biotin. b) Image of an anti-biotin affinity blot of an SDS-PAGE gel containing samples of *S. aureus* ATCC35556 pretreated with the indicated inhibitors at the specified concentrations or vehicle control before labeling with FP-biotin (5 μM). Red arrowhead and box indicate the primary target of JCP251, blue arrowhead and box indicate the primary target of JCP678. The experiment was performed twice with similar results.

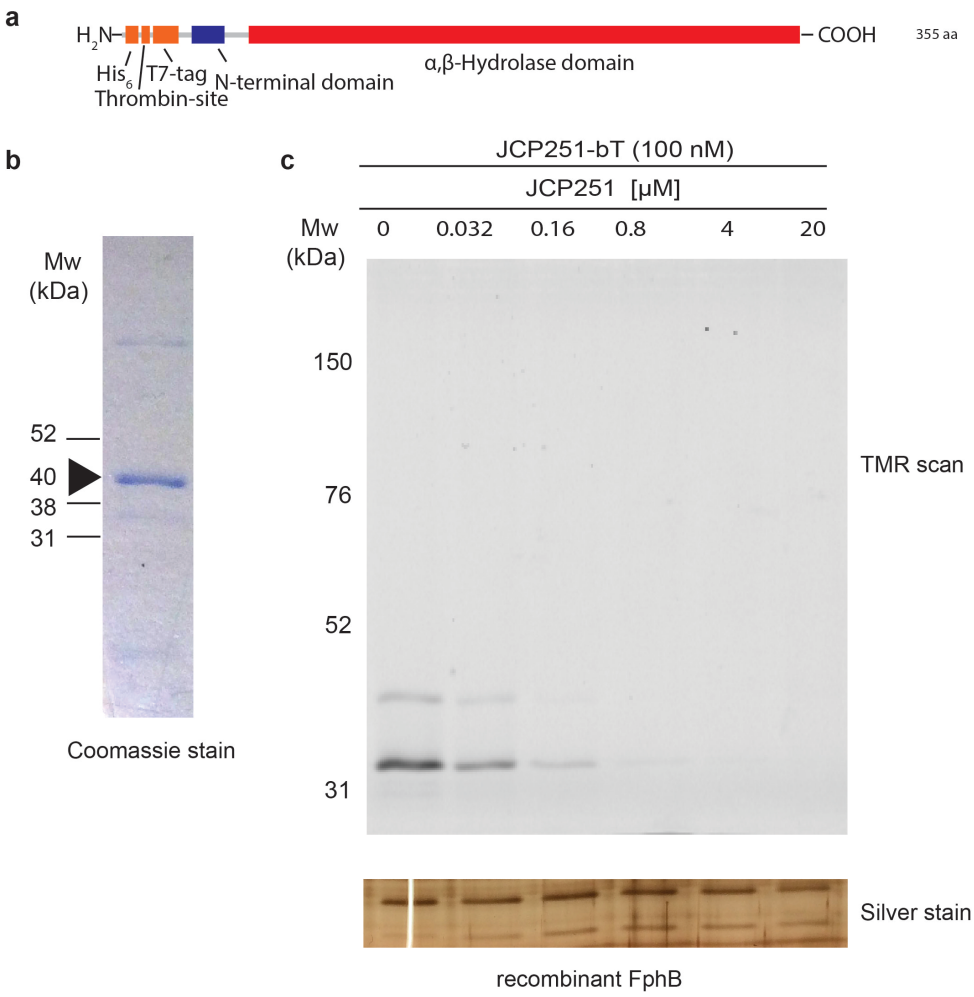

Supplementary Figure 3. Purification, ABP-labeling and functional characterization of recombinant FphB. a) Predicted protein domain overview of recombinant FphB. b) SDS-PAGE analysis of purified rFphB protein, visualized by Coomassie staining. c) SDS-PAGE analysis (TMR-scan in upper panel and silver stain as loading control in lower panel) of rFphB labeled with JCP251-bdpTMR after pre-incubation with different concentrations of JCP251. The experiments were repeated twice with similar results.

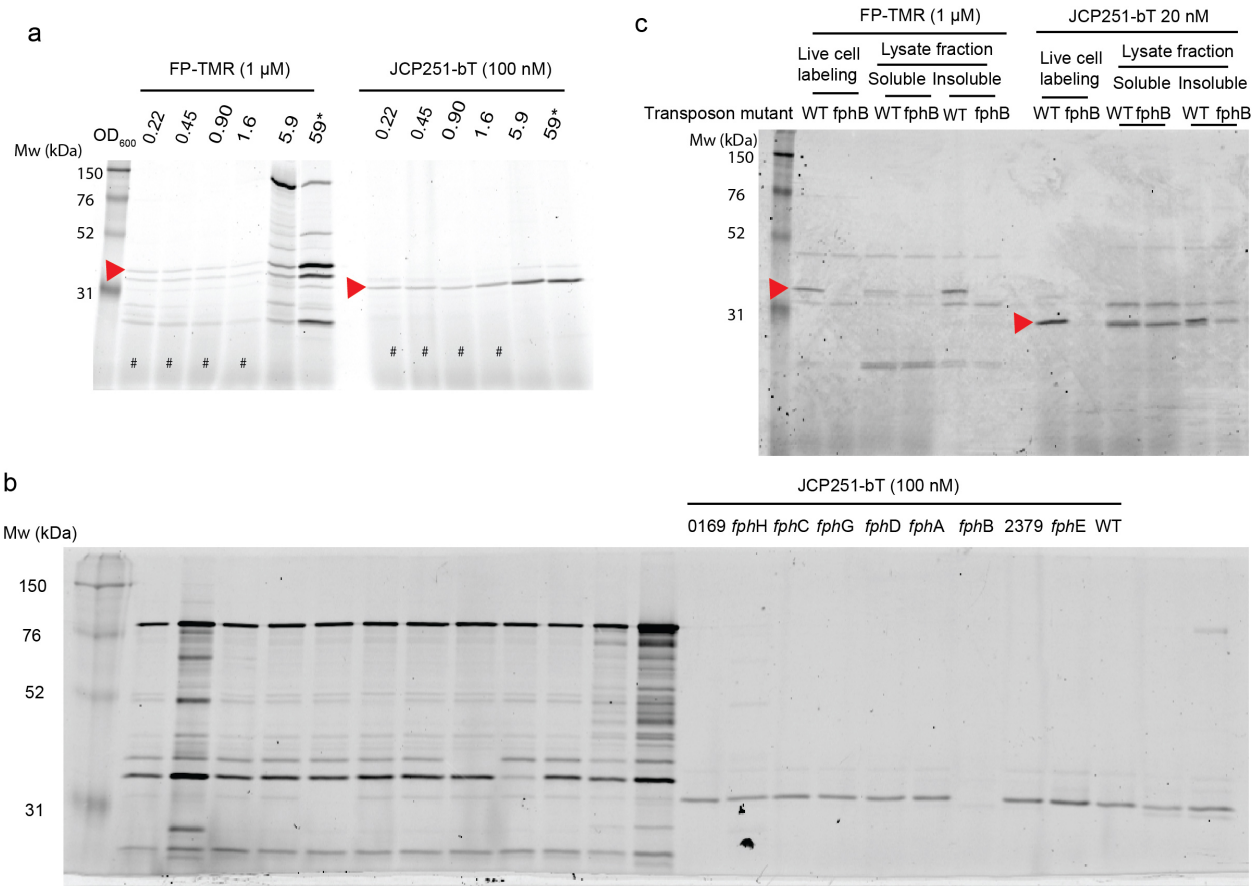

Supplementary Figure 4. Labelling of FphB throughout various growth stages in culture. a) SDS-PAGE images of *S. aureus* ATCC35556 cells grown in liquid culture during exponential (OD_{600} 0.22 – 1.6) and stationary phase (OD_{600} = 5.9) to the indicated OD_{600} and then labeled for 30 min with FP-TMR (1 μM) or JCP251-bdpTMR (100 nM). Samples were lysed and analyzed by SDS-PAGE followed by detection of TMR-fluorescence by scanning of the gel with a flatbed laser scanner. Red arrowheads indicate FphB. # indicates loading was normalized to the cell density of the most dilute sample (OD_{600}=0.22). * For OD_{600} = 59, the stationary phase culture was concentrated 10-fold. The red arrow indicates FphB. Note that the protein runs faster in the gel when labeled with JCP251-bT compared to FP-TMR. This experiment was performed once. b) SDS-PAGE fluorescence scan of indicated *S. aureus* transposon mutant strains labeled with JCP251-bT. Full gel image corresponding to Fig. 3d. c) SDS-PAGE fluorescence scan images of *S. aureus* Newman WT and *fphB*::ϕNΣ labeled as live cells or in lysate with FP-TMR or JCP251-bT. Cells were grown to mid-exponential phase and either labeled with probe as live cells or alternatively, cells were lysed and fractionated before soluble and insoluble lysate fractions were labeled with probe at the indicated concentrations. The experiment was performed twice with similar results.

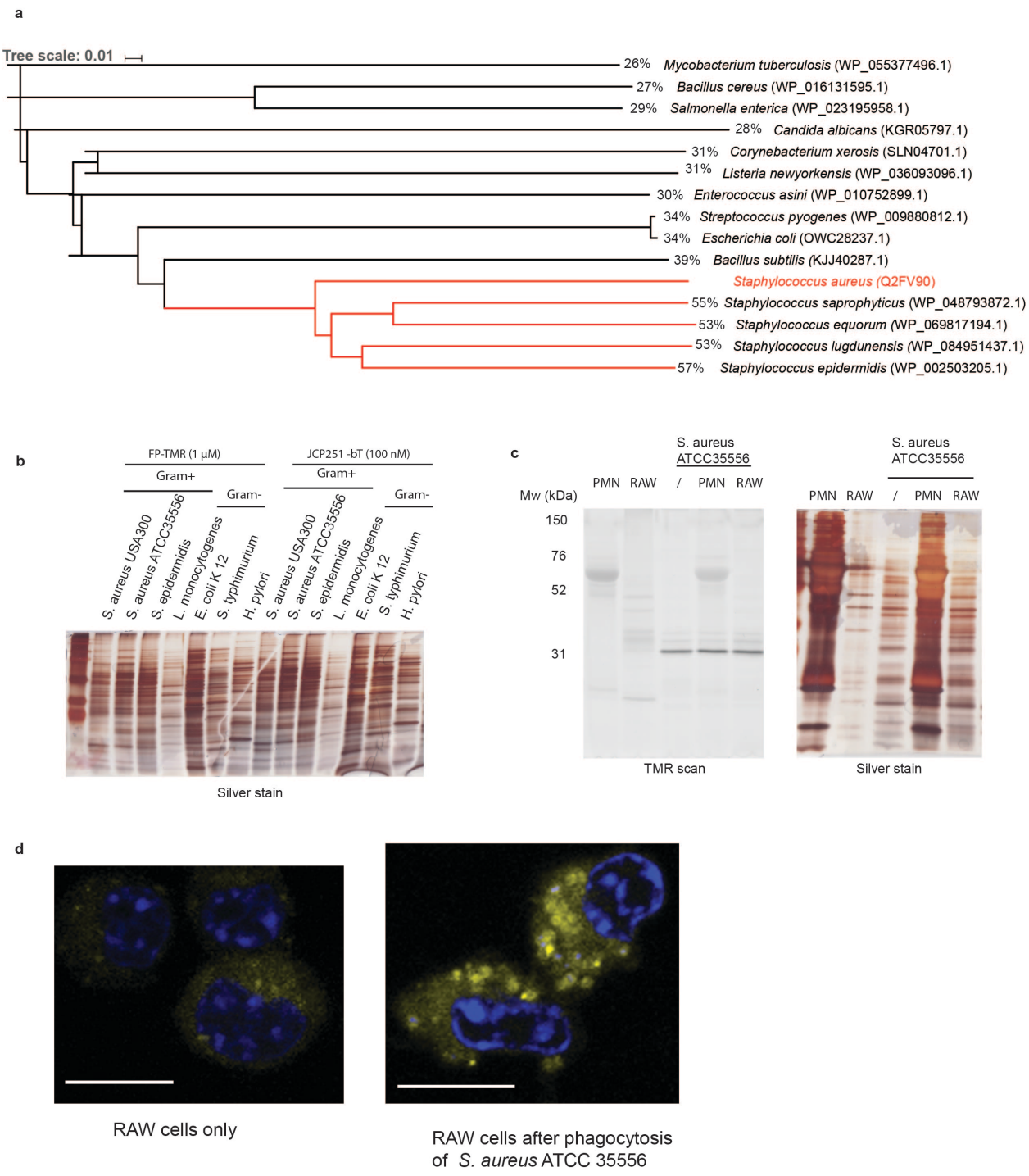

Supplementary Figure 5. Selectivity of JCP251-bdpTMR labeling. a) Phylogenetic tree showing the closest homologs of FphB in various prokaryotic and eukaryotic organisms. Homologous proteins were identified by blastp search. No homologs were found for *Homo sapiens*, *P. aeruginosa*, *H. pylori* and *Propionibacterium acnes*. Sequences were subjected to Clustal Omega Multiple Sequence Alignment and a phylogenetic tree generated using iTOL. Values between tree branches and organism names indicate % identity values compared to *S. aureus* FphB. b) Image of the silver stained SDS-PAGE gel from Fig. 2E showing bacterial pathogen lysates after labeling with fluorescent ABPs FP-TMR and JCP251-bdpTMR c) SDS-

PAGE gel of samples of peripheral mononuclear cells (PMN) purified from human blood, cells or the murine macrophage RAW cell line alone or co-cultured with *S. aureus* ATCC3556 60 min before labeling with 100 nM JCP251-bT. Samples were lysed and analyzed by SDS-PAGE and probe fluorescence visualized by scanning of the gel with a flatbed laser scanner (left) or total protein visualized by Silver stain (right). d) Confocal micrographs of RAW cells alone (left) and after phagocytosis of *S. aureus* ATCC35556 (right), labeled with 100 nM JCP251-bT. Blue: DAPI, Yellow: JCP251-bT labeling. Scale bar: 10 μm. All experiments were repeated twice with similar results.

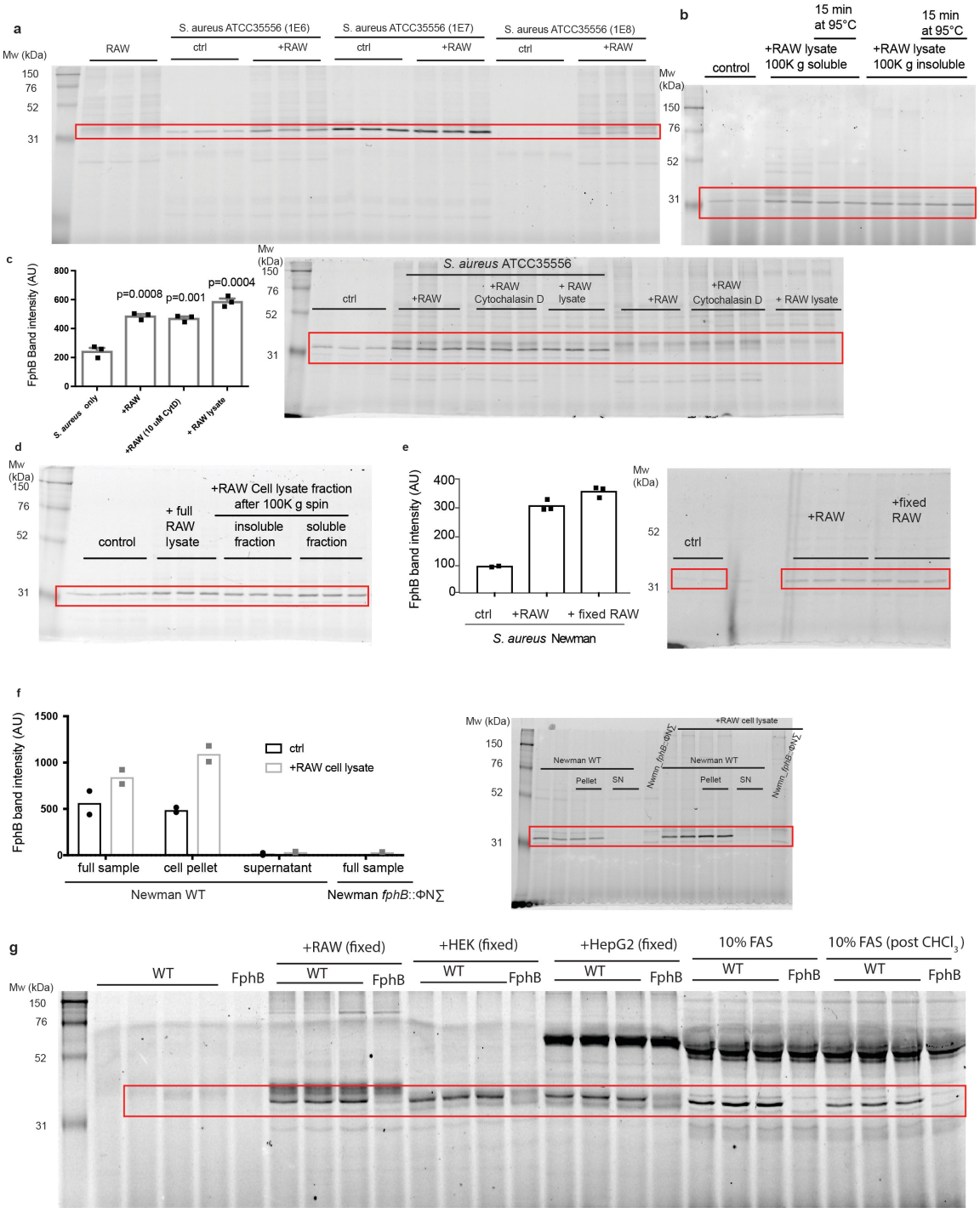

Supplementary Figure 6. Stimulatory activity of eukaryotic cell components on FphB activity.

Graphs show JCP251-bT labeling profile S. aureus cells in response to different stimuli (gel images) and quantification of FphB intensities. FphB bands are highlighted in red boxes. a) *S. aureus* ATCC35556 was incubated for 90 min at indicated CFUs in the presence or absence of RAW cells (1E5), labelled with 100 nM JCP251-bT. Gel corresponds to data shown in Fig. 4a. b) *S. aureus* ATCC35556 (1E7 CFU) was grown in the presence of full RAW cell lysate or the insoluble and soluble fractions after ultracentrifugation (each equivalent to 1E5 cells) prior to JCP251-bT labeling (Gel corresponds to data shown in Fig. 4b) c) Left: FphB band intensity after *S. aureus* ATCC35556 (1E7 CFU) were grown in the presence of RAW cells (1E5), RAW cells pretreated with 10 μM Cytochalasin D to block phagocytosis, or RAW cell lysate (equivalent of 1E5 cells) prior to JCP251-bT labeling. Graph shows means ± SD of three independent biological samples. Statistical significance was tested using unpaired, two-tailed Student's t-test. Right: Corresponding full gel image. d) *S. aureus* ATCC35556 were treated with heat-inactivated or untreated soluble/insoluble lysate fractions after ultracentrifugation prior to JCP251-bT labeling. Gel corresponds to data shown in Fig. 4c. e) Left: FphB band intensity after *S. aureus* Newman (1E7 CFU) was grown in the presence of live or PFA-fixed RAW cells prior to JCP251-bT labeling. Graph shows means ± SD of two (ctrl) or three (stimulations) independent biological samples. Right: Corresponding full gel image. f) Left: FphB band intensity after *S. aureus* Newman (1E7 CFU) were grown in the presence or absence of RAW cell lysate. After stimulation, some samples were spun down and the supernatant and cell pellet analyzed separately by SDS-PAGE analysis. Graph shows means ± SD of two independent biological samples. Right: Corresponding full gel image. g) *S. aureus* Newman WT or *fphB::*ϕNΣ mutant were incubated with PFA-fixed RAW cells, HEK cells, HepG2 cells, 10% Fetaplex™ Animal Serum Complex (FAS) or 10% FAS after chloroform extraction prior to labeling with JCP251-bT labeling. Gel corresponds to data shown in Fig. 4d. All experiments were repeated twice with similar results.

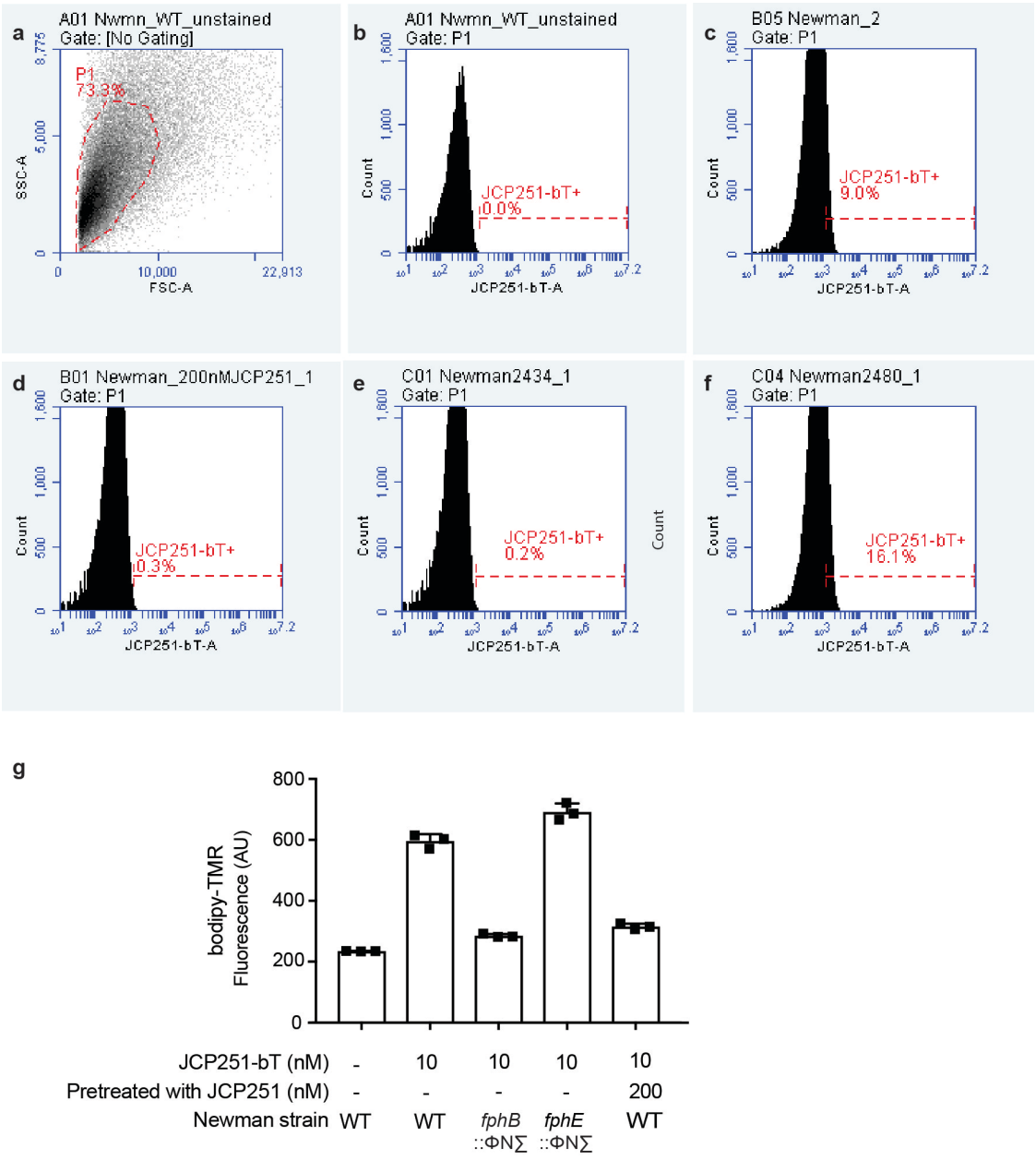

Supplementary Figure 7. Flow cytometry analysis of JCP251-bT labeling of *S. aureus*. FACS scatter plot showing the region used for gating of samples (dashed red line). a) FCS-A vs. SSC-A. Gate P1 includes bacterial cells. b) Histogram of events in the P1 gate depicting bT-fluorescence against cell count of the unstained *S. aureus* Newman WT control sample. The JCP251-bT+-gate used for analysis in Fig. 3B was set accordingly. c-f) Histograms showing bT-fluorescence of c) strain Newman WT d) strain Newman WT after preincubation with 200 nM JCP251, e) strain Newman *fphB*::ϕNΣ (Newman2434) and f) strain Newman *fph*E::ϕNΣ (Newman2480) labeled with 10 nM JCP251-bT. g) Plot of mean bT-fluorescence intensities ± SD of all cells in the P1 gate in arbitrary units from three biologically independent samples. The experiment was repeated twice with similar results.

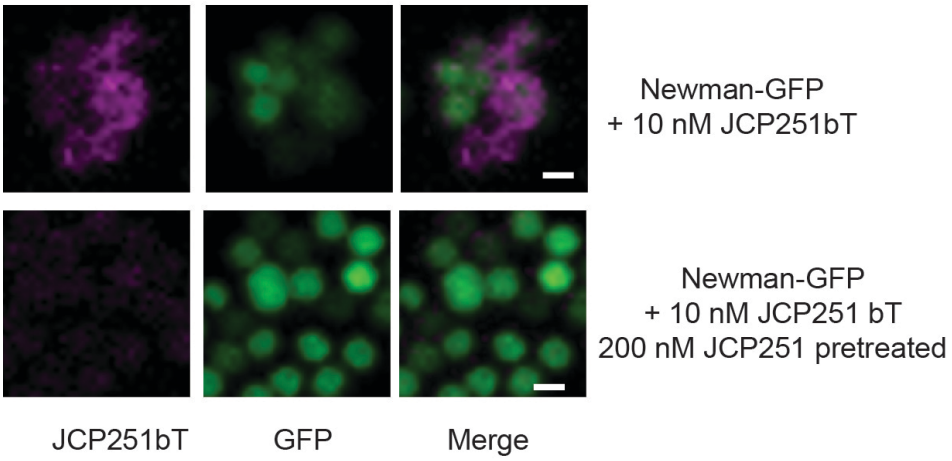

Supplementary Figure 8. Confocal micrographs of *S. aureus* Newman-GFP. Confocal micrographs of a *S. aureus* Newman-GFP expressing strain labeled with 10 nM JCP251-bT after pretreatment with 200 nM JCP251 or vehicle during exponential growth. GFP-fluorescence: green, bT-fluorescence: magenta. Scale bar: 1 μm. The experiment was repeated twice with similar results.

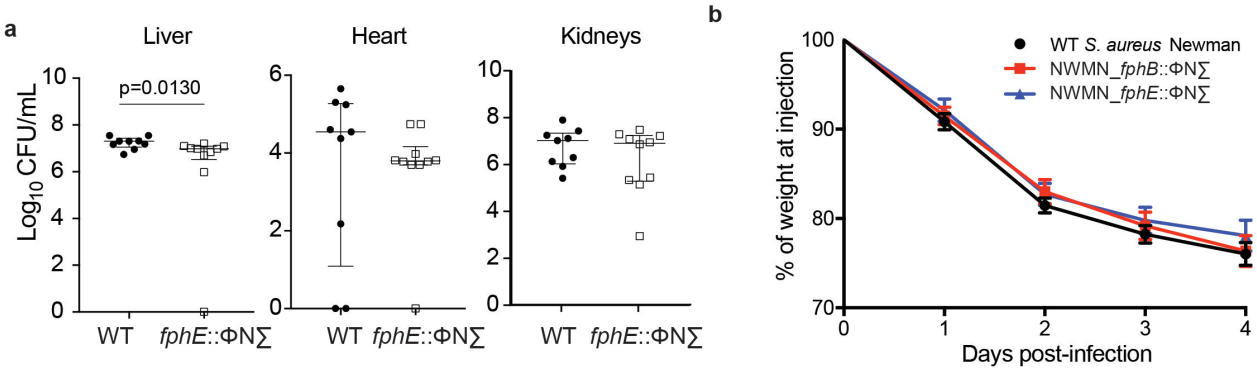

Supplementary Figure 9. Effects of loss of FphE activity on infectivity *in vivo*. a) Plots of total CFU recovered from indicated organs of BALB/c mice 96 hours after intravenous infection with *S. aureus* Newman WT or *fphE*::ϕNΣ. Graphs show pooled data (median ± interquartile range, WT:n=9, *fphE*::ϕNΣ. n=10) from 2 independent experiments. Significance was tested by two-sided Mann-Whitney test: *p<0.05. c) % Weight loss of BALB/c mice at different times post i.v. infection with *S. aureus* Newman WT, *fphB*::ϕNΣ or *fphE*::ϕNΣ mutant. Graph shows pooled data (means ± SD) from 2 independent experiments (WT, *fphB*::ϕNΣ: n=9, *fphE*::ϕNΣ: n=10).